International Journal of Signal Processing, Image Processing and Pattern Recognition
Vol.8, No.9 (2015), pp.229-238
http://dx.doi.org/10.14257/ijsip.2015.8.9.24

Brain Tumor Segmentation from Multispectral MRIs Using Sparse Representation Classification and Markov Random Field Regularization

Tianming Zhan[1], Shenghua Gu[2], Can Feng[3], Yongzhao Zhan[1] and Jin Wang[2]

1. School of Computer Science & communications Engineering, Jiangsu University, Zhenjiang 212013, China
2. Jiangsu Key Laboratory of Big Data Analysis Technology, Nanjing University of Information Science and Technology, Nanjing 210044, China.
3. Center of software, China North Industries Group Corporation Co., Ltd., Nanjing, 210044, China

Abstract

Automatic brain tumor segmentation from multispectral magnetic resonance imaging (MRI) data is an important but a challenging task because of the high diversity in the appearance of tumor tissues among different patients and in many cases similarity with the normal tissues. In this paper, we propose a fully automatic technique for brain tumor segmentation from multispectral human brain MRIs. We first use the intensities of different patches in multispectral MRIs to represent the features of both normal and abnormal tissues and generate a dictionary for following tissue classification. Then, the sparse representation classification (SRC) is applied to classify the brain tumor and normal brain tissue in the whole image. At last, the Markov random field (MRF) regularization introduces spatial constraints to the SRC to take into account the pair-wise homogeneity in terms of classification labels and multispectral voxel intensities. Our method was evaluated on 20 multi-modality patient datasets with competitive segmentation results.

Keywords: *brain tumor segmentation, multispectral MRIs, sparse representation, MRF*

1. Introduction

In the current clinical inflation, medical imaging is becoming a very important aspect for many applications from diagnosis to treatment [1]. Nowadays, various medical images such as Magnetic Resonance Imaging (MRI), Computerized Tomography (CT), Positron Emission Tomography (PET), Single-photon Emission Computerized Tomography (SPECT) etc. play an important role in process of brain tumor diagnosing and treating. Each imaging modality has its special imaging mechanism to supply different useful information. For brain tumor diagnosis and treatment, MRI has several advantages over other medical imaging modalities such as a useful non-invasive technique for assisting in clinical diagnoses [2].

In recent years, multispectral MRIs are usually used to delineate the tumor and its sub-regions in clinical practice. Different MRI sequences can respectively provide different and partly independent information about different tissues, and reflect pathologic information about the brain tumor [2]. The commonly used spectral images include T1-weighted (T1), T2-weighted (T2), T1-weighted images with contrast enhancement (T1C) and T2-FLAIR (Fluid Attenuated Inversion Recovery) weighted for brain tumor extraction. The tumor area is usually divided into necrotic, active and edema sub-regions. In general, the radiologist needs to consider all these MRIs simultaneously for brain tumor diagnosis [3]. For helping brain tumor imaging analysis, the tumor region

ISSN: 2005-4254 IJSIP

segmentation or detection is a necessary and essential step. Subsequently, a large amount of research in last few yearshas been focused on fully automatic methods for segmenting brain tumors from multispectral MRIs.

Even with multimodality MRIs, brain tumor segmentation is still a challenging task because the tumors vary greatly in size and position and have a variety of shape and appearance properties [4-5]. Therefore, it is difficult to segment a brain tumor by using a simple unsupervised threshold. For accurately segment the brain tumor, we need to explore the characteristic and pathological process of brain tumor. On this basis, many other methods have been proposed for automatically segment the brain tumor. In paper [4] and [6], these methods were divided into four groups based on their fundamental theories: (1) atlas-based method [7], (2) contour/surface evolution [8], (3) graph-based [9] and (4) learning-based [10]. Compared with these methods, a new classification method based on sparse representation theory now is wildly applied in several image classification or segmentation fields [11]. This method represents a testing sample as a sparse linear combination of atoms in an over-complete dictionary, which is built by the training samples from all classes. The label of a testing sample is determined by the representation residue with respect to each class [12]. This method assumes that data or each testing sample is independently and identically distributed and doesn't consider any spatial relationships. However, most voxel labels in medical image strongly depend on their neighbors. Therefore, we need to take the spatial relationship into account for accurate segmentation results.

In this paper, we propose a fully automatic technique by integrating the sparse representation classifier (SRC) and Markov random field (MRF) for brain tumor segmentation from multispectral human brain MRIs. We first use the intensities of different patches in multispectral MRIs to represent the features of both normal and abnormal tissues and generate a dictionary for following tissue classification. Then, the sparse representation classifier (SRC) is applied to classify the brain tumor and normal brain tissue in the whole image. At last, the Markov random field (MRF) regularization introduces spatial constraints to the SRC to take into account the pair-wise homogeneity in terms of classification labels and multi-modality voxel intensities. Our method was evaluated on 20 multi-modality patient datasets with competitive segmentation results. This paper is a revised and expanded version of a paper [19] presented at international conferences on ISA, CIA 2015 in Philippines.

2. Sparse Representation Classifier

Given a dictionary $D=[D_1, D_2, \cdots, D_k]$ which is built by all training samples, k represents the total number of class labels, and $D_i=[D_{i1}, D_{i2}, \cdots, D_{in_i}]$ represents the training samples from the *i*-th class, a testing sample *y* is assumed to be represented as a sparse linear combination of dictionary elements in D:

$$y=\alpha_{11}D_{11}+\alpha_{12}D_{12}+\cdots+\alpha_{1n_1}D_{1n_1}+\cdots+\alpha_{k1}D_{k1}+\alpha_{k2}D_{k2}+\cdots+\alpha_{kn_k}D_{1n_k} \quad (1)$$

which can be written as

$$y=D\alpha \quad (2)$$

where α contains the sparse coefficients and is usually called as sparse code.

To find the sparse representation of any test sample *y*, a coefficient vector α needs to be calculated

$$\alpha=[\alpha_{11}, \alpha_{12}, \cdots \alpha_{1n_1}, \cdots, \alpha_{k1}\alpha_{k2}, \cdots, \alpha_{kn_k}]^T \text{ Subject to } y=D\alpha \quad (3)$$

To calculate this sparsest coefficient vector we need to solve the following optimization problem:

$$\alpha_0=\arg\min\|\alpha\|_0 \text{ subject to } y=D\alpha \quad (4)$$

Where $\|\alpha\|_0$ represents the number of non-zero components in the coefficient vector α. Finding the solution to Eq. (4) is NP hard problem [13]. So the problem can be solved using *l*1-norm, which is a convex optimization problem:

$$\alpha_1 = \arg\min \|\alpha\|_1 \text{ subject to } y = D\alpha \tag{5}$$

Usually, the signals are always corrupted by noise, so we always find the sparse solution of coefficient vector α using following minimization:

$$\alpha_1 = \arg\min \|\alpha\|_1 \text{ subject to } \|D\alpha - y\|_2 \le \varepsilon \tag{6}$$

Then, the classification results can be estimated using the residual error:

$$L(y) = \arg\min_i \|y - D_i\alpha_i\| \tag{7}$$

3. Our Method

To segment a multispectral MRIs $I = \{I_{T1}, I_{T2}, I_{T1C}, I_{FL}\}$ using SRC, the intensity patch of each pixel is firstly represented as a column vector and used to construct the dictionary. Let $N(x)$ be the neighborhood of pixel x with the neighborhood size $w \times w \times w$, the feature of pixel x in T1 sequence can be represented as $v_{T1}(x)$ (its size is $w^3 \times 1$)which is transformed from the patch $N(x)$. Therefore, the feature of pixel x (its size is $4w^3 \times 1$)in multispectral MRI scan be constructed by:

$$v(x) = [v_{T1}(x); v_{T2}(x); v_{T1c}(x); v_{FL}(x)] \tag{8}$$

After that, each training data is represented to the column vector as Eq. (8) and integrated into a dictionary for brain tumor segmentation. To classify the testing pixel into different class (tissue, edema, tumor in multispectral MRIs), we use Eq. (8) to transform the neighborhood patch into a column vector, and represent it by linear sparse coding. According to the SRC description in section 2 and following [14], we estimate the coefficient vector by minimizing a non-negative Elastic-Net problem[15]:

$$\min_{\substack{\alpha \\ \alpha \ge 0}} \|D\alpha - v(x)\|_2^2 + \lambda_1 \|\alpha\|_1 + \lambda_2 \|\alpha\|_2^2 \tag{9}$$

where, the first term is the intensity vector fitting term based on the intensity patch similarity, the *l*1regularization term is used to enforce the sparse constraint of the reconstruction coefficients, and the *l*2 smoothness term is used to enforce the coefficients to be similar for the similar patch[14,15]. The details about the solution of Eq. (9) can be seen in paper [15].

After minimization of Eq. (9) for each testing pixel, the probability of each pixel belonging to different class can be estimated using the reconstruction error:

$$p_i(x) = \frac{\sum_j \|v(x) - D_j\alpha_j\|_1 - \|v(x) - D_i\alpha_i\|_1}{\sum_j \|v(x) - D_j\alpha_j\|_1} \tag{10}$$

The testing data is able to be classified by calculating the maximum of probabilities generated by Eq. (10). However, only patch intensity information is used for classification, the brain tumor segmentation performance is not good enough due to poor MR image quality. Thus, we need to use the spatial contextual information to improve the brain tumor segmentation accuracy. In our paper, the MAP-MRF framework is applied to regularize the SRC map to improve the brain tumor segmentation results. This framework encourages the classification of one pixel to depend on the labels of neighboring pixels. According to [16], the MAP segmentation in the framework of Bayesian theory is given by:

$$l^* = \arg\max_l \left\{ \sum_x \log p(l(x) \mid x) + \log p(l) \right\} \tag{11}$$

where, $l(x)$ is the label of pixel x , $p(l(x)|x)$ is the conditional probability which represents the patch intensity information. $p(l)$ is the prior probability which represents the spatial information. In this paper, $p(l(x)|x)$ is given by Eq. (10) which is generated by the reconstruction error of SRC. The spatial prior $p(l)$ is given by MLL prior as follows:

$$p(l) = \frac{1}{Z} e^{\mu \sum_{(x,y)\in C} \delta(l(x)-l(y))} \tag{12}$$

where, Z is a normalizing constant for the density, μ is a parameter that controls the level of the smoothness. The spatial prior penalizes segmentations where adjacent regions are assigned to different classes.

According to Eq. (11) and Eq. (12), the MAP segmentation is written as follows:

$$l^* = \arg\min_l \left\{ \sum_x -\log p(l(x)|x) - \mu \sum_{(x,y)\in C} \delta(l(x)-l(y)) \right\} \tag{13}$$

Minimization of (13) is a combinatorial problem involving unary and pairwise interaction terms [16-17]. In this paper, the a-Expansion graph cut algorithm [18] is applied to solve the minimization of Eq. (13).

3. Implementation and Results

We evaluate our model on the BRATS 2012 challenge data set of 20MRIs with brain tumor, 10 subjects are simulated data and other 10 subjects are real patient data. Each subject comprises T1, T2, T1C and FLAIR sequences.

Figure 1 shows two brain tumor segmentation results of real and simulated data. The first row and third row show the original images of T1, T2, FLAIR and T1C sequences respectively. We can see that the intensities of the tumor region and brain tissues are quite different in these four sequences. The second and fourth rows show the brain tumor segmentation results and corresponding ground truth. The first and second columns demonstrate the tumor segmentation using SRC method and SRC-MRF method respectively, the third columns demonstrate the ground truth, and the last column demonstrates the difference quantity between tumor segmentation by using SRC-MRF method and the ground truth. From these two results, we can see that using MRF regularization on SRC results can improve the tumor segmentation results which indicate the importance of the spatial contextual information in brain tumor segmentation for detecting the complete boundaries of tumor and reducing the influence of the noise. Also, the difference quantity images demonstrate that our segmentation results are very close to the ground truth which indicates that our method is able to obtain accurate brain tumor segmentation results.

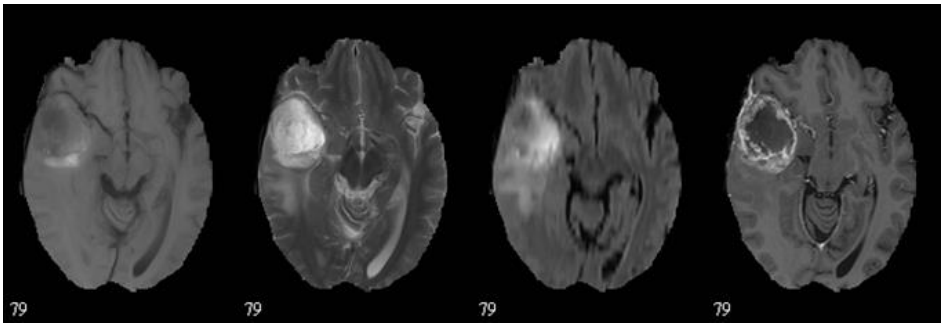

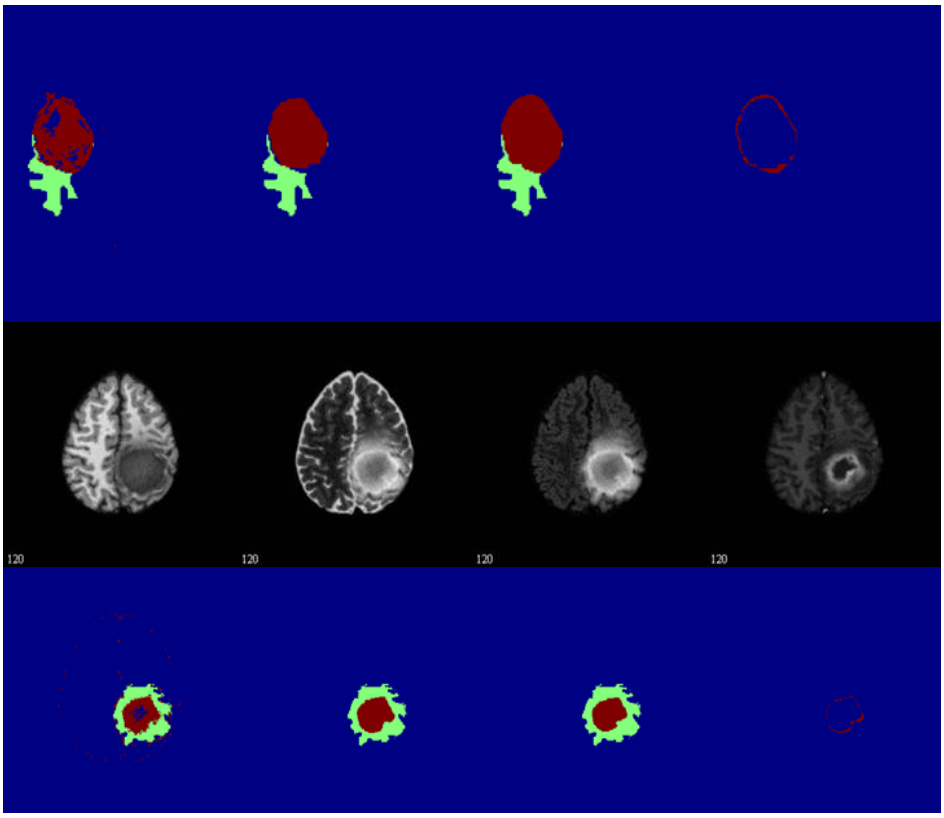

Figure 1. Two examples of the brain tumor segmentation results. The first and third rows show the original images from four different modalities: T1, T2, FLAIR and T1C images from left to right. The second and fourth rows show the segmentation results of brain tumor obtained by SRC, SRC-MRF, ground truth and the difference image between our segmentation result and the ground truth.

The brain tumor segmentation results of our algorithm for a real patient and simulated 3D data is shown in Figure 2. The first row shows four T2 images from different slices of one 3D real patient data. The segmentation results of our algorithm are demonstrated in the second row. The third row shows the corresponding segmentation of brain tumor provided by expert radiologist and used only for performance evaluation and comparison. Four T1C images from different slices of one 3D simulated data are shown in fourth row, the fifth and last row demonstrate our segmentation results and ground truth, respectively. By comparing to the ground truth given by expert radiologist, it is clear that our brain tumor segmentation results show a high similarity to the ground truth which demonstrates the efficacy of our method for 3D brain tumor multispectral MRIs segmentation.

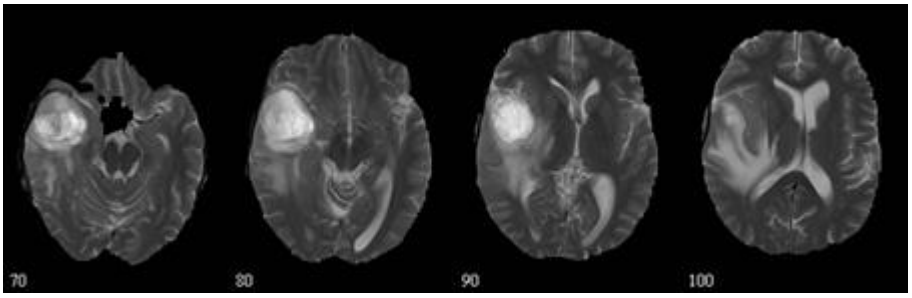

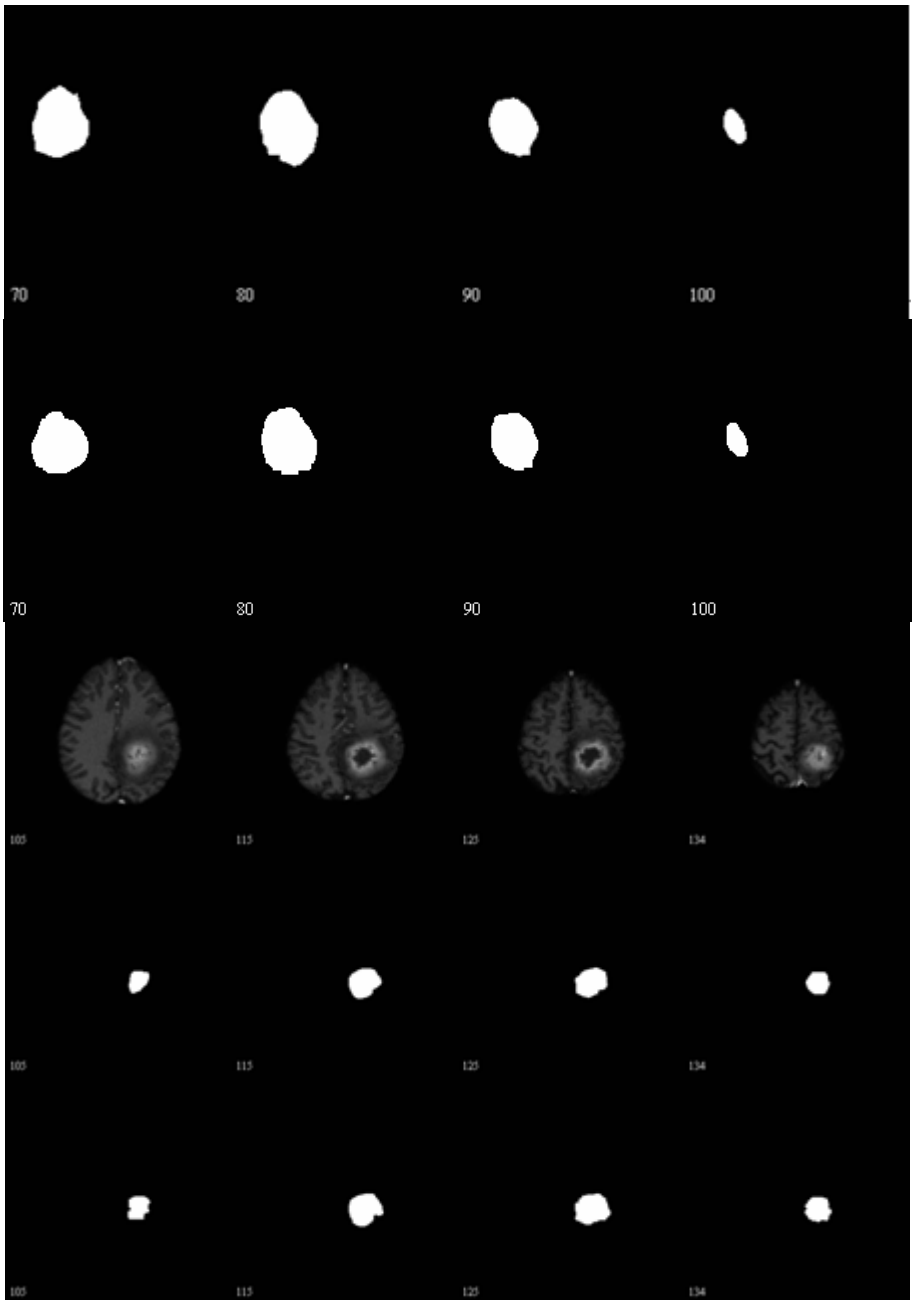

Figure 2. Two example of 3D brain tumor segmentation. First row: the T2 images of different slices from a real patient subject. Second row: Segmentation results produced by our algorithm. Third row: manual segmentation obtained by a radiologist. Fourth row: the T1C images of different slices from a simulated subject. Fifth row: Segmentation results produced by our algorithm. Last row: manual segmentation obtained by a radiologist.

We employed the Jaccard score to quantitatively evaluate the segmentation results obtained by the multinomial logistic regression (MLR), SRC, MLR-MRF as well as our SRC-MRF method in 20 subjects. Table 1 demonstrates the Jaccard Score of these four methods on simulated data and real data. As shown in these two tables, the mean Jaccard score value of the results obtained by MLR, SRC, MLR-MRF and our SRC-MRF method executed on simulated data and real data are 0.80, 0.82, 0.87, 0.93, and 0.61, 0.67, 0.75,

0.82, respectively. We can see that the Jaccard scores of SRC are higher than those of MLR classifier, which indicated that the performance of SRC is much better than that of MLR classifier. The Jaccard scores of results obtained by these two classifiers with MRF regularization are both higher than those of results obtained by the two classifiers without MRF regularization which show significant improvements by encouraging the spatial information to improve the segmentation accuracy. Besides this, the Jaccard scores of the results obtained by our method are highest which demonstrate the efficiency and competitiveness of our method.

Table 1. Jaccard Score of Each Method for the 10 Simulated Subjects

		MLR	SRC	MLR-MRF	SRC-MRF
Real data	Subject 1	0.80	0.84	0.87	0.88
	Subject 2	0.74	0.74	0.80	0.85
	Subject 3	0.58	0.60	0.70	0.76
	Subject 4	0.55	0.63	0.75	0.78
	Subject 5	0.51	0.58	0.73	0.74
	Subject 6	0.62	0.64	0.72	0.83
	Subject 7	0.68	0.71	0.75	0.85
	Subject 8	0.52	0.65	0.70	0.87
	Subject 9	0.54	0.63	0.71	0.78
	Subject 10	0.56	0.68	0.77	0.86
	Average	**0.61**	**0.67**	**0.75**	**0.82**
Simulated Data	Subject 1	0.88	0.90	0.91	0.97
	Subject 2	0.86	0.86	0.90	0.95
	Subject 3	0.76	0.83	0.85	0.94
	Subject 4	0.74	0.78	0.86	0.95
	Subject 5	0.85	0.83	0.88	0.91
	Subject 6	0.81	0.82	0.85	0.88
	Subject 7	0.76	0.80	0.85	0.90
	Subject 8	0.77	0.80	0.85	0.93
	Subject 9	0.82	0.82	0.90	0.93
	Subject 10	0.75	0.78	0.85	0.94
	Average	**0.80**	**0.82**	**0.87**	**0.93**

4. Conclusion

In this paper, we presented a novel brain tumor segmentation method by using sparse representation classifier and Markov random filed regularization. We first use the intensities of different patches in multispectral MRIs to represent the features of both normal and abnormal tissues and generate a dictionary for following tissue classification. Then, the sparse representation classification (SRC) is applied to classify the brain tumor and normal brain tissue in the whole image. At last, the Markov random field (MRF) regularization introduces spatial constraints to the SRC to take into account the pair-wise homogeneity in terms of classification labels and multispectral voxel intensities. Our method was evaluated on 20 BRATS challenge subjects; the higher Jaccard Score values demonstrate the advantage and considerable competence of our method.

Acknowledgements

This paper is a revised and expanded version of a paper entitled "Brain Tumor Segmentation from multispectral MRIs Using Sparse Representation Classification and Markov Random Field Regularization" presented at CST 2015, Suzhou, China, April 23-25, 2015. This work is supported by the Chinese Postdoctoral Science Foundation Funded

Project (No.2014M561587), Natural Science Foundation of Jiangsu Province (No.BY2014007-04) Natural Science Foundation of Universities in Jiangsu Province (No.13KJB520016), Jiangsu Postdoctoral Science Foundation Funded Project (No.1402094C), Research Foundation for Talented Scholars, Jiangsu University (No.14JDG041), National Natural Science Foundation of China (614022342).

5. References

5.1. Journal Articles

[1] N. Singh and Naveen Chodhary. A review of brain tumor segmentation and detection techniques through MRI, International Journal of Computer Application, 2014, vol. 103(7): 8975-8887.
[2] N. Zhang, S. Ruan, S. Lebonvallet, Q. Liao and Y. Zhu, "Key feature selection to fuse multi-spectral MRI images for brain tumor segmentation", Computer Vision and Image Understanding, vol. 115, (**2011**), pp. 256-269.
[4] J. Jiang, Y. Wu, M. Huang, W. Yang, W. Chen and Q. Feng, , "3D brain tumor segmentation in multimodal MR images based on learning population-and patient-specific feature sets", Computerized Medical Imaging and Graphics, vol. 37, no. 7, (**2013**), pp. 512-521.
[5] K. Popuri, "3D variational brain tumor segmentation using Dirichlet priors on a clustered feature set", International journal of computer assisted radiology and surgery, vol. 7, no, 4, (**2012**), pp. 493-506.
[6] N. Gordillo, E. Montseny and P. Sobrevilla, "State of the art survey on MRI brain tumor segmentation", Magnetic resonance imaging, vol. 31, no. 8, (**2013**), pp. 1426-1438.
[11] K. Huang and S. Adviser-Aviyente, "Sparse representations for image classification", Michigan State University, (**2007**).
[13] H. Zou and T. Hastie, "Regularization and variable selection via the elastic net", Journal of the Royal Statistical Society: Series B (Statistical Methodology), vol. 67, no. 2, (**2005**), pp. 301-320.
[14] L. Wang, F. Shi and Y. Gao, "Integration of sparse multi-modality representation and anatomical constraint for isointense infant brain MR image segmentation", NeuroImage, vol. 89, (2014), pp. 152-164.
[15] H. Zou and T. Hastie, "Regularization and variable selection via the Elastic Net", J. R. Stat. Soc. Ser. B, vol. 67, (**2005**), pp. 301-320.
[16] J. Li, J. M. Bioucas-Dias, and A. Plaza, "Spectral–spatial hyperspectral image segmentation using subspace multinomial logistic regression and Markov random fields", IEEE Trans. Geosci. Remote Sens., vol. 50, no. 3, (**2012**), pp. 809–823.
[17] Y. Tarabalka, "SVM- and MRF-Based Method for Accurate Classification of Hyperspectral Images", IEEE Geoscience and Remote Sensing Letters, vol. 7, no. 4, (**2010**), pp. 736-740.
[18] Y. Boykov and V. Kolmogorov, "An experimental comparison of mincut/max-flow algorithms for energy minimization in vision", IEEE Trans. Pattern Anal. Mach. Intell., vol. 26, no,. 9, (**2004**), pp. 1124–113.
[19] J. Wang, J.-U. Kim, L. Shu, Y. Niu and S. Lee, "A distance-based energy aware routing algorithm for wireless sensor networks", Sensors, vol. 10, no. 10, (**2010**), pp. 9493-9511.
[20] J. Wang, Y. Yin, J. Zhang, S. Lee, and R. S. Sherratt, "Mobility based energy efficient and multi-sink algorithms for consumer home networks", IEEE Transactions on Consumer Electronics, vol. 59, no. 1, (**201**3) February, pp.77-84.
[21] R. Hong, J. Pan, S. Hao, M. Wang, F. Xue and X. Wu, "Image quality assessment based on matching pursuit", Inf. Sci., (**2014**), pp. 196-211.
[22] R. Hong, W. Cao, J. Pang and J. Jiang, "Directional projection based image fusion quality metric", Inf. Sci., (**2014**), pp. 611-619.

5.2. Conference Proceedings

[3] S. Bauer, L.-P. Nolte and M. Reyes, "Fully automatic segmentation of brain tumor images using support vector machine classification in combination with hierarchical conditional random field regularization", Medical Image Computing and Computer-Assisted Intervention–MICCAI 2011, Springer Berlin Heidelberg, (**2011**), pp. 354-361.
[7] B. Menze, K. Van Leemput, D. Lashkari, MA. Weber, N. Ayache and P. Golland, "A generative model for brain tumor segmentation in multi-modal images", In: Medical image computing and computer-assisted intervention – MICCAI, (**2010**), pp. 151–159.
[8] A. Lefohn, J. Cates and R. Whitaker, "Interactive, GPU-based level sets for 3Dsegmentation", In: Ellis R, Peters T, editors. Medical image computing and computer-assisted intervention – MICCAI 2003, lecture notesin computer science, vol. 2878. Berlin/Heidelberg: Springer; (**2003**), pp. 564-572.
[9] N. Birkbeck, D. Cobzas, M. Jagersand, A. Murtha and T. Kesztyues, "An interactive graph cut method for brain tumor segmentation", In: Presented at workshop on applications of computer vision (WACV), (**2009**), pp. 1-7.

[10] J. Zhang, KK. Ma, MH. Er and V. Chong, "Tumor segmentation from magnetic resonance imaging by learning via one-class support vector machine", In: Presented at international workshop on advanced image technology (IWAIT'04), (**2004**), pp. 207-211.
[12] Q. S. ulHaq, "Hyperspectral data classification via sparse representation in homotopy", Information Science and Engineering (ICISE), 2010 2nd International Conference on. IEEE, (**2010**), pp. 3748-3752.
[19] T. Zhan, S. Gu, C. Feng and Y. Zhan, "Brain Tumor Segmentation from multispectral MRIs Using Sparse Representation Classification and Markov Random Field Regularization", Proceedings of international conferences on ISA, CIA 2015, Philippines.

Authors

Tianming Zhan, he received his Ph.D. degree in Pattern recognition and intelligent system from Nanjing University of Science & Technology in 2013. His main research interests include image processing, medical image analysis, pattern recognition and numerical analysis.

Shenghua Gu, Research assistant of Jiangsu Key Laboratory of Big Data Analysis Technology, Nanjing University of Information Science and Technology. His main research interests include image processing, pattern recognition.

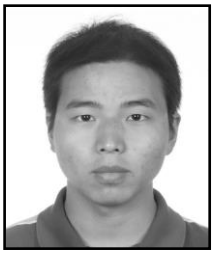

Can Feng, he received his Ph.D. degree in Pattern recognition and intelligent system from Nanjing University of Science & Technology in 2013. He is currently an Engineer in North Information Control Group Co., Ltd., China. His research interests include image processing, medical image analysis, compressive sensing and its application in image processing.

Yongzhao Zhan, he is a professor and Ph. D Supervisor of School of Computer Science and Communication Engineering, Jiangsu University. His research interests include Human Computer Interaction, Distributed Computing, Image and Video Processing.